IOWA STATE UNIVERSITY
Digital Repository

Materials Science and Engineering Publications | Materials Science and Engineering

8-22-2018

Drying mediated orientation and assembly structure of amphiphilic Janus particles

Kyle Miller
Iowa State University, kylem167@iastate.edu

Ayuna Tsyrenova
Iowa State University, ayuna@iastate.edu

Stephen M. Anthony
Sandia National Laboratories

Shiyi Qin
Binghamton University

Xin Yong
Binghamton University

See next page for additional authors

Follow this and additional works at: https://lib.dr.iastate.edu/mse_pubs

 Part of the Polymer and Organic Materials Commons

The complete bibliographic information for this item can be found at https://lib.dr.iastate.edu/mse_pubs/383. For information on how to cite this item, please visit http://lib.dr.iastate.edu/howtocite.html.

This Article is brought to you for free and open access by the Materials Science and Engineering at Iowa State University Digital Repository. It has been accepted for inclusion in Materials Science and Engineering Publications by an authorized administrator of Iowa State University Digital Repository. For more information, please contact digirep@iastate.edu.

Drying mediated orientation and assembly structure of amphiphilic Janus particles

Abstract

Amphiphilic Janus particles demonstrate unique assembly structures when dried on a hydrophilic substrate. Particle orientations are influenced by amphiphilicity and Janus balance. A three-stage model is developed to describe the process. Simulation further indicates the dominant force is capillary attraction due to the interface pinning at rough Janus boundaries.

Disciplines

Materials Science and Engineering | Polymer and Organic Materials

Comments

This is a manuscript of an article published as Miller, Kyle, Ayuna Tsyrenova, Stephen M. Anthony, Shiyi Qin, Xin Yong, and Shan Jiang. "Drying mediated orientation and assembly structure of amphiphilic Janus particles." *Soft Matter* 14, no. 33 (2018): 6793-6798. DOI: 10.1039/c8sm01147h. Posted with permission.

Authors

Kyle Miller, Ayuna Tsyrenova, Stephen M. Anthony, Shiyi Qin, Xin Yong, and Shan Jiang

This article is available at Iowa State University Digital Repository: https://lib.dr.iastate.edu/mse_pubs/383

This paper describes objective technical results and analysis. Any subjective views or opinions that might be expressed in the paper do not necessarily represent the views of the U.S. Department of Energy or the United States Government.

SAND2018-10053J

Drying Mediated Orientation and Assembly Structure of Amphiphilic Janus Particles

Kyle Miller,[a†] Ayuna Tsyrenova,[a] Stephen M. Anthony,[b] Shiyi Qin,[c] Xin Yong*[c] and Shan Jiang*[ad]

[a] *Department of Materials Science and Engineering, Iowa State University, Ames, IA 50011, USA. E-mail: sjiang1@iastate.edu*

[b] *Department of Bioenergy and Defense Technology, Sandia National Laboratories, Albuquerque, NM, USA*

[c] *Department of Mechanical Engineering and Institute for Materials Research, Binghamton University, Binghamton, NY, 13902, USA. E-mail: xyong@binghamton.edu*

[d] *Division of Materials Science & Engineering, Ames National Laboratory, Ames, IA 50011, USA*

† Electronic supplementary information (ESI) available.

Abstract

Amphiphilic Janus particles demonstrate unique assembly structures when dried on a hydrophilic substrate. Particle orientations are influenced by amphiphilicity and Janus balance. A three-stage model is developed to describe the process. Simulation further indicates the dominant force is capillary attraction due to the interface pinning at rough Janus boundaries.

Sandia National Laboratories is a multimission laboratory managed and operated by National Technology & Engineering Solutions of Sandia, LLC, a wholly owned subsidiary of Honeywell International Inc., for the U.S. Department of Energy's National Nuclear Security Administration under contract DE-NA0003525.

The drying of colloidal suspensions is a ubiquitous process in nature and everyday life. Many commercial applications, including printing and coating products,[1,2] rely on drying to form a coherent thin film that adheres to the substrate. Furthermore, the ability to fabricate functional thin films via a simple drying process will help address challenges in cutting-edge applications such as flexible electronics, bio-sensing, and multifunctional coatings.[3–5] From a fundamental perspective, the drying process usually involves fast dynamics that are far from equilibrium. In addition, the liquid-gas interface further complicates the transport, interaction, and assembly of the colloidal constituents during the process. Previous studies have revealed interesting patterns driven by evaporation. The prime example is the "coffee ring" commonly observed in drying sessile droplets.[6] However, most of the studies have only focused on homogeneous or isotropic particles and their spatial distribution. No systematic studies, in either experiment or simulation, have reported how structured particles, such as Janus particles, where two sides of the particles are made of different chemical compositions, self-assemble during the drying process.

More importantly, the anisotropy of Janus particles elicits a completely new question regarding particle orientation, which does not exist for conventional isotropic particles. Orientation is also associated with anisotropic molecules such as surfactants, proteins, and di-block copolymers. Studies have shown that drying conditions can drastically affect the assembly and orientation of these molecules and even induce different phase behaviors.[7–9] Beyond the molecular system, Janus nanoparticles and nanoclusters demonstrate unique assembly structures both in bulk and at interfaces.[10,11] However, the assembly and orientation of Janus particles at much larger length scales (μm) under the drying conditions have not been extensively studied. Due to the anisotropy of interactions and amphiphilicity of Janus particles, their interactions among each other and with interfaces are completely different from homogeneous particles. The interface and the drying process will play a significant role in controlling the assembly and orientation of Janus particles. This report offers a new model system in both experiment and simulation for providing insight into the unique behavior of anisotropic building blocks. Furthermore, the orientation of Janus particles is a critical consideration for their functionality, as it directly affects the material properties of the dried film.[4]

In this report, we examined the translational and rotational dynamics of Janus particles during the drying process. Particle orientation was analyzed using an image analysis algorithm on scanning

electron microscope (SEM) images, which show contrast between the coated sides. We propose a three-stage model to describe the drying process of Janus particles. We discovered that the orientations and assembly structures of Janus particles are affected by both amphiphilicity and Janus balance (geometry) of spheres. Additionally, particle orientation is highly coupled with aggregation structures. A coarse-grained simulation with explicit solvent was developed to reveal the fundamental interactions between particles during drying. Capillary attraction was induced by the pinning of contact line around the rough boundaries on Janus particles. This force is found to dominate the interactions and leads to unique deposition patterns.

Janus particles were fabricated following a protocol developed previously.[12] Experimental details can be found in ESI. Au (top layer) was deposited onto a monolayer of 3 μm silica particles. Thiol molecules are then used to render Au surface with different chemical properties. ODT (1-octadecanethiol) and DDT (1-Dodecanethiol) are used to render Au surface hydrophobic and obtain amphiphilic Janus particles (JP-ODT and JP-DDT), while MHA (16-Mercaptohexadecanoic acid) is used to give the Au surface a negative charge (JP-MHA). To obtain Janus particles of different Janus balance, coated Janus particles were etched by aqua regia solution. Control particles (JP-SiO_2), which are optically Janus however chemically homogeneous, were obtained by depositing another layer of silica onto the Au coated particle monolayer instead of the thiol treatment.

For the drying experiment, we only used hydrophilic glass substrate cleaned by O_2 plasma. The drying process was imaged in real time via an optical microscope. The details of dried particle assembly were imaged using SEM. Both backscattered and secondary electron images were taken and fed into an algorithm (ESI) developed to extract orientation of Janus particles.

For computer simulations of evaporating colloidal films, we performed many-body dissipative particle dynamics (MDPD)[13–16] to probe competing interactions that drive the self-assembly of Janus particles. MDPD models solvent and Janus particles explicitly by representing a volume of fluid or solid as individual coarse-grained beads, whose dynamics is governed by classical mechanics. Similar to standard dissipative particle dynamics (DPD),[17–19] MDPD captures hydrodynamics in colloidal suspensions. However, different from DPD, which can model only single-phase fluid or density-matching binary fluid, MDPD is capable of modeling multiphase fluid with large density and viscosity contrast, e.g., liquid-vapor coexistence (Fig. 3). Thus, the

drying process can be explicitly simulated using MDPD. Evaporation is modeled by reducing the vapor density below the saturation vapor density through continuous removal of vapor beads following a procedure described in our previous work.[20] Colloidal particles are modeled as non-deformable clusters of frozen MDPD beads translating and rotating as rigid bodies.[21–23] The particle bead density is adjusted to prevent the penetration between solvent beads and particles. In addition, since adsorption energy is magnitudes higher than the gravity energy associated with center of weight shift due to the gold coating in experiment, the density of gold is not considered in the simulation. The surface chemistry of particle is readily controlled by tuning the interaction parameters of the constituent beads.[24–26] Janus boundary roughness is introduced as a sinusoidal perturbation with amplitude δ_r as shown in Fig. S1. Simulation details are described in ESI.

Drying of colloidal suspensions is a complicated process. Similar studies have focused on the lateral distribution of isotropic particles, namely the coffee ring effect due to evaporation-induced capillary flow.[6] We also observed coffee ring formed by Janus particles, which is beyond the scope of this report. Instead, we emphasize the unique orientation and local monolayer assembly of a dilute solution of Janus particles mediated by the drying process.

Fig. 1 clearly shows the assembly structure and particle orientation after solution is completely dried. The bright side is Au coated side. For Janus particles, almost all the particles orient with the Au side facing towards the air, with out-of-plane angle (θ) (Fig. S2) very close to 0° (Fig. 1a). For homogeneous particles, obviously orientation should be random, which is clearly demonstrated by control particles JP-SiO_2 in Fig. 1b. Particle tracking results shown in Figs. 1c&d further confirmed the observation quantitatively. The orientation preference for larger angles for control particles is likely due to the high density of Au coating, which directs particles to orient more towards the substrate.

Interestingly, Janus particles form a large-scale open fractal structure while homogeneous particles only show small aggregates. In separate experiments, the deposits of JP-ODT and JP-DDT showed very similar structures when dried under the same conditions, while JP-MHA resembles the homogeneous particles (Fig. S3). We note that both ODT and DDT are hydrophobic ligands, while MHA is negatively charged. The results indicate that the fractal structures were formed due to the amphiphilicity of Janus particles. In addition, the fractal cluster

structures suggest that the assembly is limited by diffusion and Janus particles may experience strong attractions during the drying process.

Real-time video revealed the detailed dynamics of the drying process. The snapshots in Fig. 2 suggest the drying process has three stages. In Stage I, Janus particles adsorb onto the air-water interface as the water surface recedes towards the substrate; in Stage II Janus particles quickly aggregate into cluster structures; in Stage III, the aggregates further assemble as water evaporates away and assembly structures are eventually deposited onto the substrate. The particle aggregation pattern is consistent with the Janus particle assembly structures formed at the interface. In Fig. 2 particles adsorbed at the interface showed a much darker color, which is due to the Au side orienting completely towards the air and blocking most of the transmitted light compared to freely rotating particles.

Another interesting observation is that Stage I and II almost happen simultaneously. This indicates again the strong attractions between Janus particles adsorbed at the interface. Notably, both the silica side of the Janus particles and the substrate are negatively charged, yet repulsive electrostatic interaction is not dominant. Although it is difficult to quantify, we consistently observed that particles with fewer neighbors are more likely to orient randomly. This suggests that the clustering of Janus particles is responsible for maintaining the orientation of particles during the Stage III of the drying process.

Previous studies have reported on that the amphiphilic Janus spheres may experience strong attraction at fluid interfaces due to the capillary force.[27] Because of imperfections in fabrication, the Janus boundary possesses certain roughness that distorts the pinned water-air interface. The hypothesis is that when water pins at the rough boundary, strong attraction is induced between particles to minimize the total surface free energy. Since it is very hard to measure and quantify the roughness of Janus boundaries experimentally, we carried out computer simulations to further study the particle interactions during the drying process. A simulation consists of an equilibrium stage to probe the self-assembly of particle at the interface in Stage II and a drying stage to reveal the final deposit in Stage III. Fig. 3 shows that Janus particles adsorb strongly at the liquid-vapor interface with their orientation fixed, while the hydrophilic homogeneous particles are dispersed uniformly in the film with random orientation. MDPD simulations allow us to directly characterize the effect of Janus boundary roughness. The “rough” Janus particles

with prescribed sinusoidal boundaries assemble into a single fractal cluster at the interface, which is reminiscent of the assembly structures observed in the experiments. Upon complete evaporation of solvent, the large cluster maintains its fractal structure and Janus particle orientation is unchanged (Movie S1). In contrast, despite having the fixed orientation, the "perfect" Janus particles with smooth Janus boundaries do not exhibit long-range ordering at equilibrium. Even with the assistance of capillary bridges between particles at the final stage of drying (see Movie S2), only small aggregates can be observed in Fig. 3b. This comparison highlights the critical role of the Janus boundary roughness.

Another observation in simulation is that the homogeneous particles also form a large cluster with random orientations after drying (see Fig. 3c). This assembly is solely induced by capillary interactions in the final drying stage when water film thickness drops below single particle diameter. Hydrophilic particles significantly deform the interface as shown in Movie S3, leading to larger attractive forces. The discrepancy between simulation and experiment is mainly due to negligible substrate friction and smaller inter-particle distances of control particles in the simulation, which promote large-scale aggregation.

We quantitatively characterize the roughness-induced effective attractions between a particle pair (see ESI for details). Fig. 3d confirms the interfacial distortion induced by the rough Janus boundary and the consequent long-range capillary attractions between particles. The strength of capillary force increases as the roughness increases. In addition, the strength is sensitive to the actual morphology of the Janus boundary, which is manifested by the amplitude of roughness and the particle radius in our simulations. Nevertheless, simulation with large particles $R_p = 10$ with rough Janus boundaries shows similar fractal aggregates (Fig. S4), confirming that the capillary attraction leads to unique large-scale assembly. Notably, a small roughness ($\delta_r = 1$) comparable to the interfacial thickness[20] fails to induce attraction. This is because in this situation the pinning induced distortion is too small to withstand the intrinsic thermal fluctuations of the interface. We did not attempt to fit the simulation results to the well-known power law $F: r^{-5}$,[28] since the sinusoidal roughness does not necessarily reproduce the quadrupolar distortion of the contact line in the experiments.[29]

In experiment, we further studied the drying pattern of Janus particles with different Janus balance. The Au coating on particles can be gradually etched away as shown in Fig. 4. The etched Janus particles have a smaller hydrophobic patch, and the size of the patch can be fine-tuned by controlling the etching time. An angle α as defined in Fig. 4a is used to characterize the geometry of Janus spheres, with $\alpha = 90°$ for un-etched particles. A series of amphiphilic Janus particles with different Janus balance were dried under the same conditions. Fig. 5d shows that Janus balance can affect the particle orientation. When $\alpha < 60°$, particles orient more randomly, and the assembly structures are small, closely packed aggregates. The structure is very similar to homogeneous particles. However, when $\alpha > 70°$, most particles orient their hydrophobic side towards air ($\theta < 30°$) and form a fractal assembly. The observation can be well explained by the capillary attraction suggested by simulation. Roughness at the boundary can still be responsible for the strong attraction for slightly etched particles ($\alpha > 70°$). However, when Au coating patch becomes very small ($\alpha < 60°$), the water contact line on adjacent particles are too far away from each other to induce strong enough attraction.

In conclusion, amphiphilic Janus particles orient with the hydrophobic side facing towards air and form fractal assembly structures when dried on a hydrophilic substrate. We further discovered that the orientation depends on the amphiphilicity and Janus balance. The orientation is maintained due to the aggregation formed when Janus particles adsorb at the water-air interface. The structures suggest that Janus particles experience strong attractions when adsorbed at interface. Computer simulations reproduced the drying process and provide convincing evidence that the strong capillary attraction induced by the pinning of the interface at the rough Janus boundaries dominates the system. If the Janus particle boundaries are completely smooth, no strong attraction was observed in the simulation.

This research is the first step in understanding the drying process involved with Janus particles. It reveals the unique physics associated with Janus spheres. The study also lays out the foundation of using Janus particles as coating materials to effectively change the surface properties. The tools developed here can serve as platform technologies for image analysis of Janus spheres and simulation of drying process.

Acknowledgement: The experiment part of this work was supported by Iowa State University Start-up Fund, and 3M Non-tenured Faculty Award. The simulation part of this work was

partially supported by the American Chemical Society Petroleum Research Fund under grant No. 56884-DNI9 and used resources of the Center for Functional Nanomaterials, which is a U.S. DOE Office of Science Facility, at Brookhaven National Laboratory under contract no. DE-SC0012704. This paper describes objective technical results and analysis. Any subjective views or opinions that might be expressed in the paper do not necessarily represent the views of the U.S. Department of Energy or the United States Government. Sandia National Laboratories is a multimission laboratory managed and operated by National Technology & Engineering Solutions of Sandia, LLC, a wholly owned subsidiary of Honeywell International Inc., for the U.S. Department of Energy's National Nuclear Security Administration under contract DE-NA0003525.

References

(1) De Gans, B.-J.; Schubert, U. S. Inkjet Printing of Well-Defined Polymer Dots and Arrays. *Langmuir* **2004**, *20* (18), 7789–7793.

(2) Steward, P. A.; Hearn, J.; Wilkinson, M. C. An Overview of Polymer Latex Film Formation and Properties. *Adv. Colloid Interface Sci.* **2000**, *86* (3), 195–267.

(3) Smalyukh, I. I.; Zribi, O. V; Butler, J. C.; Lavrentovich, O. D.; Wong, G. C. L. Structure and Dynamics of Liquid Crystalline Pattern Formation in Drying Droplets of DNA. *Phys. Rev. Lett.* **2006**, *96* (17), 177801.

(4) Jiang, S.; Van Dyk, A.; Maurice, A.; Bohling, J.; Fasano, D.; Brownell, S. Design Colloidal Particle Morphology and Self-Assembly for Coating Applications. *Chem. Soc. Rev.* **2017**, *46* (12), 3792–3807.

(5) Bigioni, T. P.; Lin, X. M. TP Bigioni, XM Lin, TT Nguyen, EI Corwin, TA Witten, and HM Jaeger, Nat. Mater. 5, 265 (2006). *Nat. Mater.* **2006**, *5*, 265.

(6) Deegan, R. D.; Bakajin, O.; Dupont, T. F.; Huber, G.; Nagel, S. R.; Witten, T. A. Capillary Flow as the Cause of Ring Stains from Dried Liquid Drops. *Nature* **1997**, *389* (6653), 827.

(7) Doshi, D. A.; Gibaud, A.; Liu, N.; Sturmayr, D.; Malanoski, A. P.; Dunphy, D. R.; Chen, H.; Narayanan, S.; MacPhee, A.; Wang, J. In-Situ X-Ray Scattering Study of Continuous Silica−Surfactant Self-Assembly during Steady-State Dip Coating. *J. Phys. Chem. B* **2003**, *107* (31), 7683–7688.

(8) Le Brun, A. P.; Chow, J.; Bax, D. V; Nelson, A.; Weiss, A. S.; James, M. Molecular Orientation of Tropoelastin Is Determined by Surface Hydrophobicity. *Biomacromolecules* **2012**, *13* (2), 379–386.

(9) Zhang, J.; Posselt, D.; Smilgies, D.-M.; Perlich, J.; Kyriakos, K.; Jaksch, S.; Papadakis, C. M. Lamellar Diblock Copolymer Thin Films during Solvent Vapor Annealing Studied by GISAXS: Different Behavior of Parallel and Perpendicular Lamellae. *Macromolecules* **2014**, *47* (16), 5711–5718.

(10) Liu, Z.; Guo, R.; Xu, G.; Huang, Z.; Yan, L.-T. Entropy-Mediated Mechanical Response of the

Interfacial Nanoparticle Patterning. *Nano Lett.* **2014**, *14* (12), 6910–6916.

(11) Ma, C.; Wu, H.; Huang, Z.; Guo, R.; Hu, M.; Kübel, C.; Yan, L.; Wang, W. A Filled-Honeycomb-Structured Crystal Formed by Self-Assembly of a Janus Polyoxometalate–Silsesquioxane (POM–POSS) Co-Cluster. *Angew. Chemie Int. Ed.* **2015**, *54* (52), 15699–15704.

(12) Jiang, S.; Yan, J.; Whitmer, J. K.; Anthony, S. M.; Luijten, E.; Granick, S. Orientationally Glassy Crystals of Janus Spheres. *Phys. Rev. Lett.* **2014**, *112* (21), 218301.

(13) Pagonabarraga, I.; Frenkel, D. Dissipative Particle Dynamics for Interacting Systems. *J. Chem. Phys.* **2001**, *115*, 5015.

(14) Trofimov, S. Y.; Nies, E. L. F.; Michels, M. A. J. Thermodynamic Consistency in Dissipative Particle Dynamics Simulations of Strongly Nonideal Liquids and Liquid Mixtures. *J. Chem. Phys.* **2002**, *117*, 9383–9394.

(15) Warren, P. B. Vapor-Liquid Coexistence in Many-Body Dissipative Particle Dynamics. *Phys. Rev. E* **2003**, *68*, 066702.

(16) Arienti, M.; Pan, W.; Li, X.; Karniadakis, G. Many-Body Dissipative Particle Dynamics Simulation of Liquid/Vapor and Liquid/Solid Interactions. *J. Chem. Phys.* **2011**, *134* (20), 204114.

(17) Hoogerbrugge, P. J.; Koelman, J. M. V. A. Simulating Microscopic Hydrodynamic Phenomena with Dissipative Particle Dynamics. *Epl* **1992**, *19* (3), 155–160.

(18) Espanol, P.; Warren, P. Statistical Mechanics of Dissipative Particle Dynamics. *Epl* **1995**, *30* (4), 191–196.

(19) Groot, R. D.; Warren, P. B. Dissipative Particle Dynamics: Bridging the Gap between Atomistic and Mesoscopic Simulation. *J. Chem. Phys.* **1997**, *107* (11), 4423–4435.

(20) Yong, X.; Qin, S.; Singler, T. J. Nanoparticle-Mediated Evaporation at Liquid–vapor Interfaces. *Extrem. Mech. Lett.* **2016**, *7*, 90–103.

(21) Chen, S.; Phan-Thien, N.; Khoo, B. C.; Fan, X. J. Flow around Spheres by Dissipative Particle Dynamics. *Phys. Fluids* **2006**, *18* (10), 103605.

(22) Fan, H.; Striolo, A. Mechanistic Study of Droplets Coalescence in Pickering Emulsions. *Soft Matter*. 2012, p 9533.

(23) Yong, X. Modeling the Assembly of Polymer-Grafted Nanoparticles at Oil-Water Interfaces. *Langmuir* **2015**, *31*, 11458–11469.

(24) Salib, I.; Yong, X.; Crabb, E. J.; Moellers, N. M.; McFarlin, G. T.; Kuksenok, O.; Balazs, A. C. Harnessing Fluid-Driven Vesicles to Pick up and Drop off Janus Particles. *ACS Nano* **2013**, *7*, 1224–1238.

(25) Yong, X.; Crabb, E. J.; Moellers, N. M.; Balazs, A. C. Self-Healing Vesicles Deposit Lipid-Coated Janus Particles into Nanoscopic Trenches. *Langmuir* **2013**, *29*, 16066–16074.

(26) Warren, P. B. No-Go Theorem in Many-Body Dissipative Particle Dynamics. *Phys. Rev. E* **2013**, *87* (4), 045303.

(27) Kumar, A.; Park, B. J.; Tu, F.; Lee, D. Amphiphilic Janus Particles at Fluid Interfaces. *Soft Matter* **2013**, *9* (29), 6604–6617.

(28) Liu, I. B.; Sharifi-Mood, N.; Stebe, K. J. Capillary Assembly of Colloids: Interactions on Planar

and Curved Interfaces. *Annu. Rev. Condens. Matter Phys.* **2018**, *9* (1), 283–305.

(29) Park, B. J.; Brugarolas, T.; Lee, D. Janus Particles at an Oil–water Interface. *Soft Matter* **2011**, *7* (14), 6413.

Figures

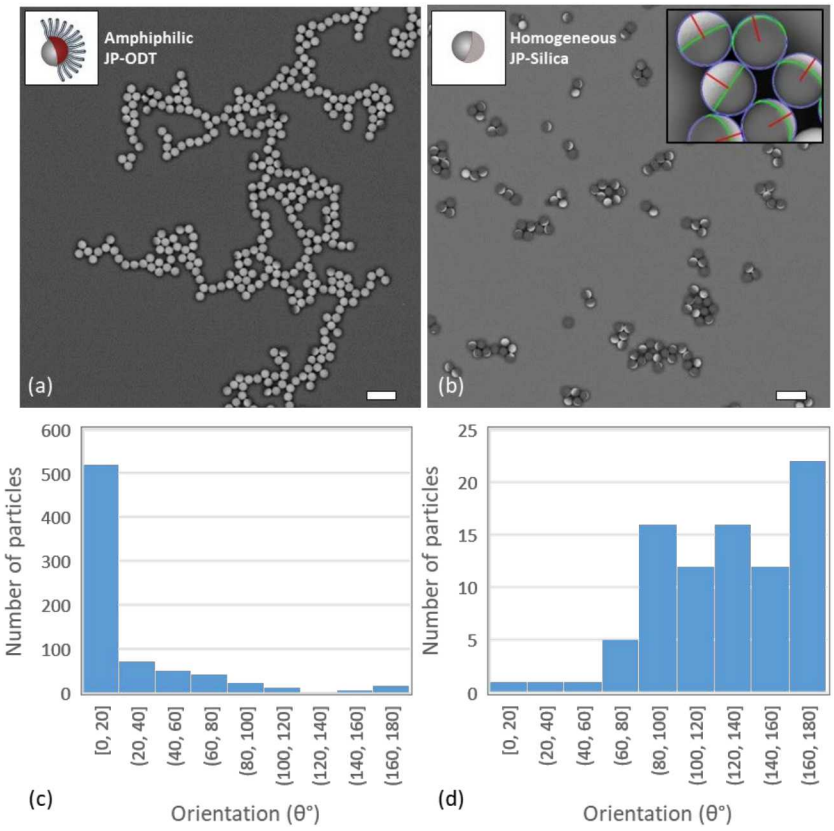

Fig. 1 SEM images and orientation analysis of dried particles on hydrophilic silicon wafer: (a) amphiphilic Janus particles; (b) homogeneous control particles, inset in the upper right corner indicates the image analysis of particle orientation; (c) orientation analysis of amphiphilic Janus particles (d) orientation analysis of homogeneous control particles.

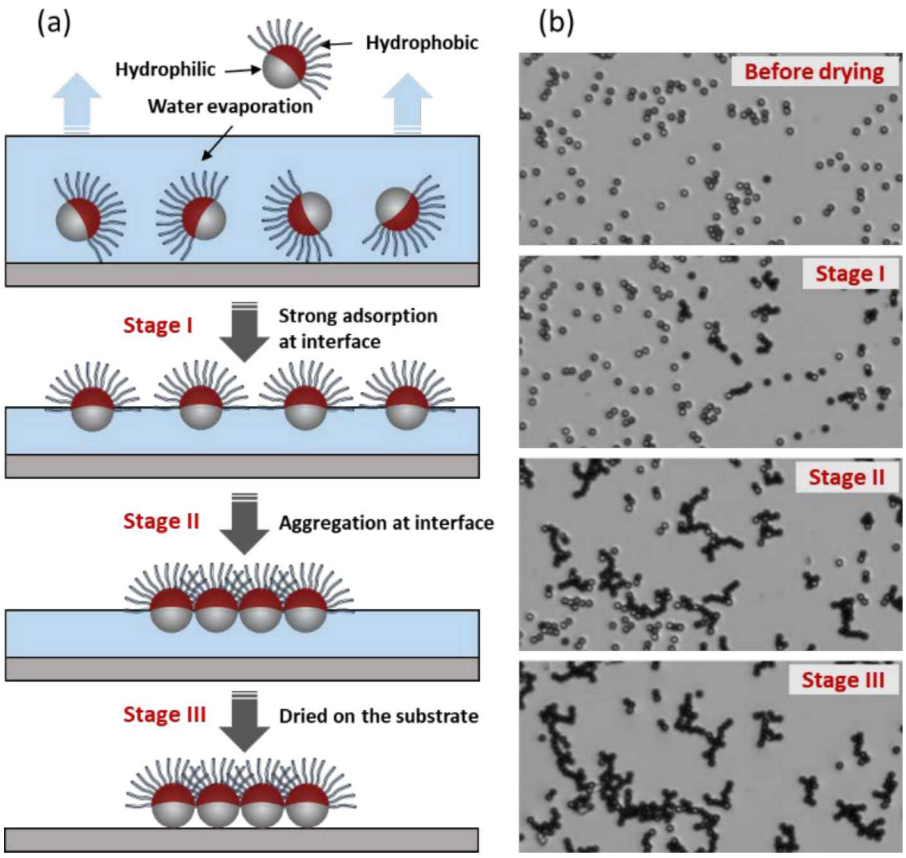

Fig. 2 Three-stage drying process: (a) schematic plot; (b) Optical microscope images of different drying stages.

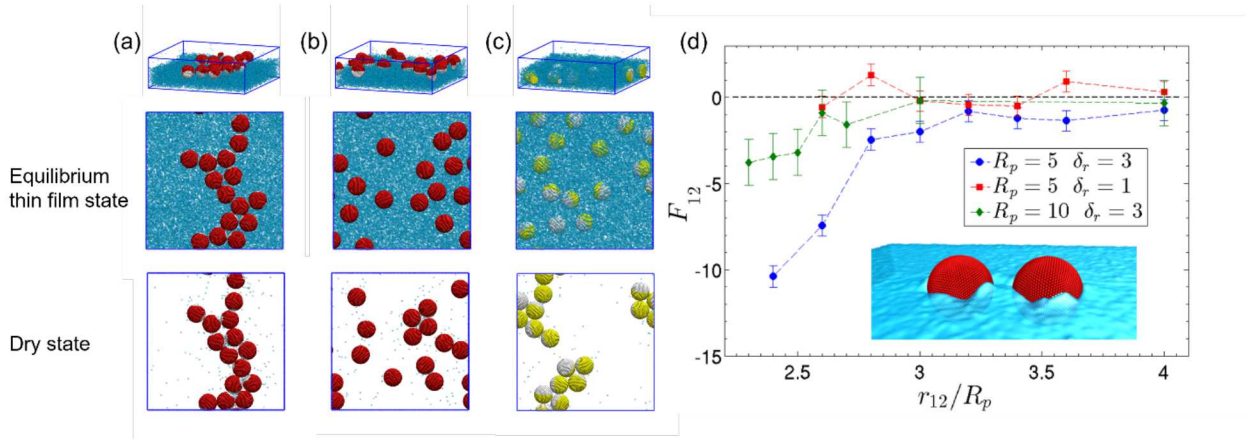

Fig. 3 Representative simulation snapshots of the assembly structures of (a) amphiphilic particles with rough Janus boundaries, (b) amphiphilic particles with smooth Janus boundaries, and (c) homogeneous control particles. (d) Effective interaction force between two amphiphilic Janus particles with rough boundaries. Negative magnitude corresponds to attraction. Error bars represent standard deviations in time. The inset shows the time-averaged interfacial distortion induced by the Janus boundary roughness of adsorbed amphiphilic particles ($R_p = 10$ and $\delta_r = 3$).

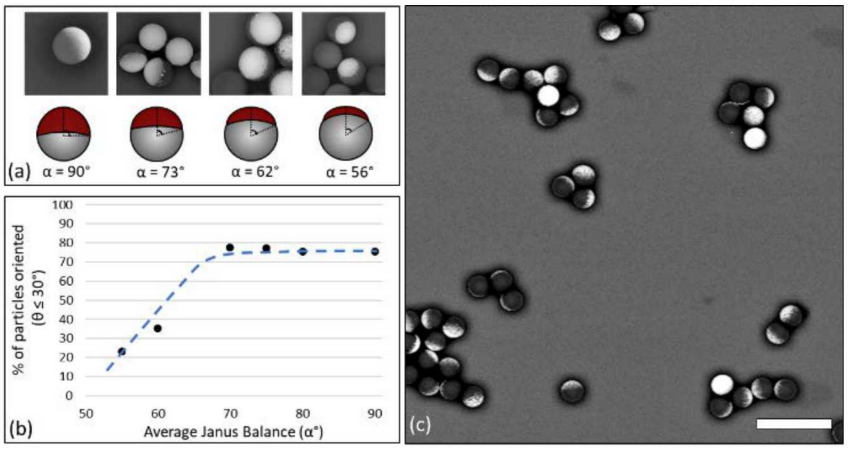

Fig. 4 Orientation and assembly affected by Janus balance: (a) Janus particles with different Janus balance synthesized by Au etching; (b) Orientation versus different Janus balance; (c) SEM images of Janus particle assembly when α = 62°.